

# ERS2 Microwave Radiometer Assessment Report

**Cycle 089**

**21-10-2003 – 24-11-2003**

Prepared by :	M. DEDIEU, CETP L. EYMARD, CETP C. MARIMONT, CETP E. OBLIGIS, CLS N. TRAN, CLS	
Checked by :	L. EYMARD, CETP	
Approved by :	P. FEMENIAS, ESA	



## Contents

<b>1</b>	<b>Introduction</b>	<b>2</b>
<b>2</b>	<b>Maps of the brightness temperatures over South Pole</b>	<b>3</b>
<b>3</b>	<b>Monitoring of the radiometer internal parameters</b>	<b>5</b>
<b>4</b>	<b>Monitoring of cold ocean brightness temperatures</b>	<b>10</b>
<b>5</b>	<b>Conclusion on the cycle assessment and long term monitoring</b>	<b>13</b>
<b>6</b>	<b>Reference documents</b>	<b>14</b>

# 1 Introduction

This document aims at reporting the behavior of ERS Microwave Radiometer in terms of instrumental characteristics and quality of the brightness temperatures. It is performed on the MWR level 0 data product (EMWC). The decoding and the pre-processing are done with the MWR level 1B reference processing chain located at CETP. The data are from the Kiruna station (KS), the Maspalomas Station (MS), the Prince Albert Station (PS) and the Gatineau Station (GS).

The objectives of this document are :

- to provide an instrumental status
- to check the stability of the instrument
- to report any change at the instrumental level likely to impact quality of the brightness temperatures

It is divided into the following topics:

- **Maps of the brightness temperatures over South Pole**
- **Monitoring of the radiometer internal parameters**
- **Monitoring of cold ocean brightness temperatures**
- **Conclusion on the cycle assessment and long term monitoring**

WARNING: As announced by the agency, due to a failure of the ERS-2 tape recorder on 22 June 2003 the recording capabilities are permanently unavailable. The ERS-2 tape recorders were used to record the ERS-2 Low Rate mission globally, after 8 years of continuous acquisition this service is now discontinued. The ERS-2 Low Rate mission will be continued within the visibility of ESA ground stations over Europe, North Atlantic, the Arctic and western North America. ESA has the intention to extend the coverage of Real Time Low Rate acquisition over the North Atlantic in the near future.

The monitoring is kept going with the remaining available data.

## 2 Maps of the brightness temperatures over South Pole

Over poles, the space and time coverages are sufficient to draw maps of the brightness temperatures. Since the atmospheric variability is weak due to the very low water vapour content, the brightness temperatures are mainly representative of surface emissivity and temperature variations, which slowly vary within the course of the year. Consequently, the south pole can be used as a stable target to monitor the brightness temperature variations with time.

Figures 1 (top) and (bottom) show respectively the 23.8 and 36.5 GHz brightness temperatures measured by the radiometer over the South pole (latitudes higher than 65°S) for the current cycle. The ice cap appears colder than the sea ice and the free water at the two frequencies.

THESE FIGURES ARE NO MORE AVAILABLE DUE TO THE PROBLEM CITED IN THE ABOVE SECTION.

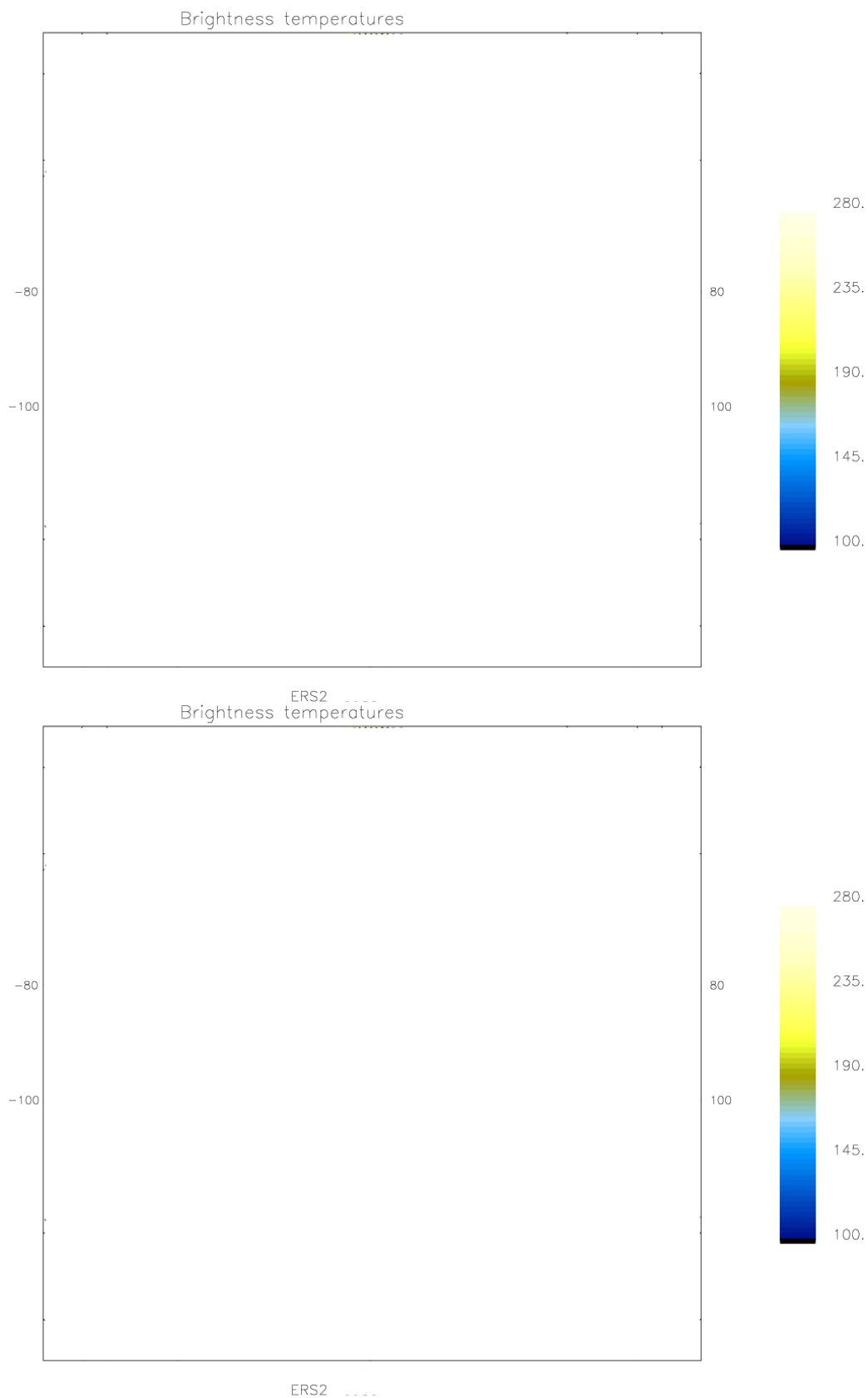


Figure 1: Brightness temperature maps over the South Pole for the two frequencies, 23.8 and 36.5 GHz.

### 3 Monitoring of the radiometer internal parameters

The radiometer telemetry primarily contains the radiometer counts for each channel, which are related to the brightness temperatures of the main antenna and the two calibration loads, through the working model (Bernard et al, 1993) summarized below:

$$\mathbf{Tfc} = acc \ ah0 \ \mathbf{TC} + (1 - acc) \ ah0 \ \mathbf{Tcc} + (1 - ah0) \ \mathbf{Th}$$

$$\mathbf{G} = (Cc - Cf) / [ao + af \ \mathbf{Tfc} - ac \ \mathbf{Tc} + ah \ \mathbf{Th}/c]$$

$$\mathbf{TE} = (Cc - off) / \mathbf{G} - aref \ \mathbf{Tref} - ad \ \mathbf{Td} + a2 \ \mathbf{Tfc} + a3 \ \mathbf{Th}/c + a4 \ \mathbf{Tc} + a6 \ \mathbf{Tcal} + a5$$

$$\mathbf{T'a} = b1 \ \mathbf{Tref} + b2 \ \mathbf{Td} - b3 \ \mathbf{Tcal} - b4 \ \mathbf{Tc} + \mathbf{TE} - (Ca - off) / \mathbf{G}$$

$$\mathbf{Ta} = c1 \ \mathbf{T'a} - c2 \ \mathbf{Tr}$$

where the coefficients are derived from the primary coefficients shown in figure 2. The brightness temperature is then derived from the antenna measurement, by accounting for the reflector losses and side lobe contributions.

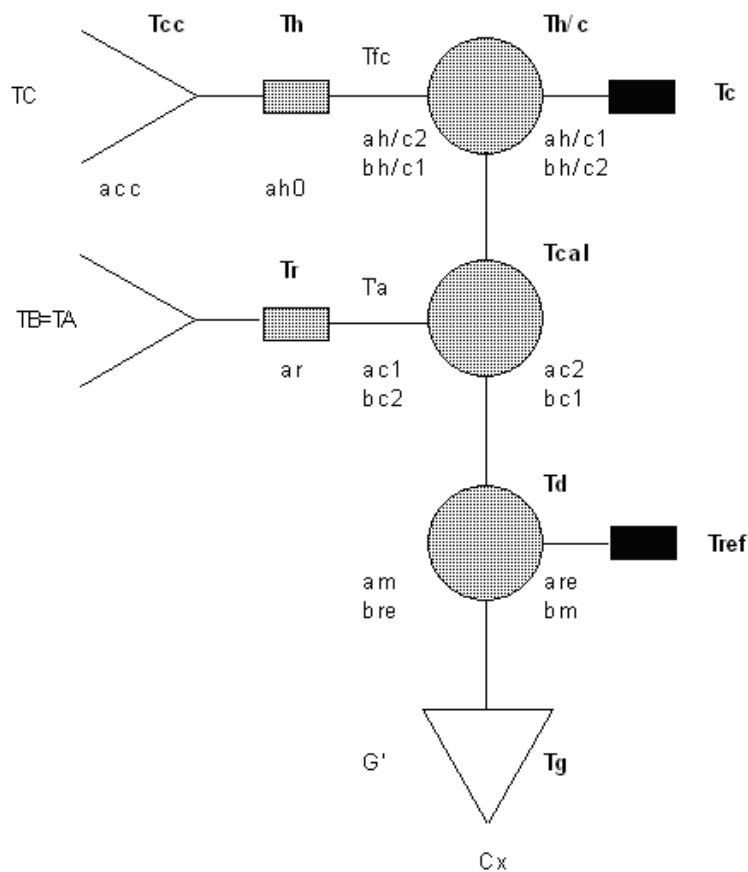


Figure 2: scheme of one channel of the MWR, showing the main antenna, whose measurement is TA, the two calibration loads, consisting of an internal hot load and a sky horn, the reference load (Dicke load - temperature Tref) and internal switches to get every measurement. Each component is characterized by transmission and loss factors which are taken into account in the radiometer model, as well as their temperature.

To monitor the instrument behaviour during its lifetime, the key parameters are plotted in figures 3-5 : gain (after correction of the thermal variations, modeled as a parabolic function),

hot load and sky horn counts, and residual term TE (residual temperature contribution due to errors in the estimated coefficients). The instrument stability is ensured if none of these parameters do vary with time.

The different plots show gaps in the monitoring due to the problem with the tape recorder.

The figure 3 (top) shows the gains of the two channels 23.8 and 36.5 GHz, after multiplying the 23.8 GHz gain by 10, and figure 3 (bottom) is a zoom on the last 10% of time. They show that the gain is very stable on both channels, despite the strong anomaly which occurred on channel 1 (23.8 GHz) in June, 1996. Since this failure the gain on this channel has been stabilized at approximately one tenth of its original value. Note that, a slow trend can be detected on calibration counts and on the residual temperature for both channels.

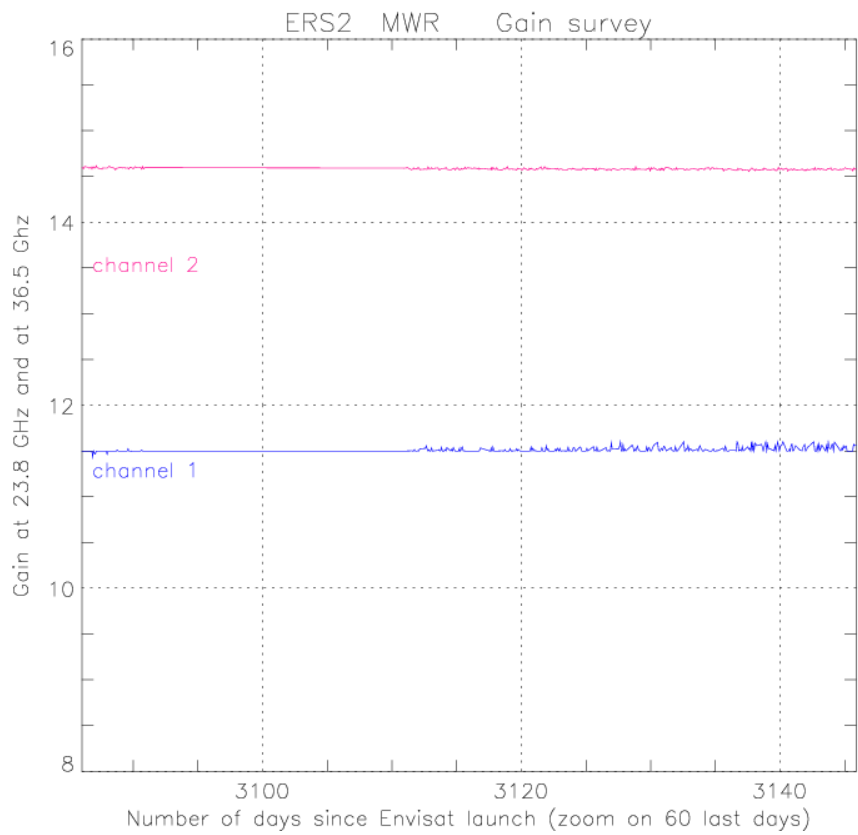
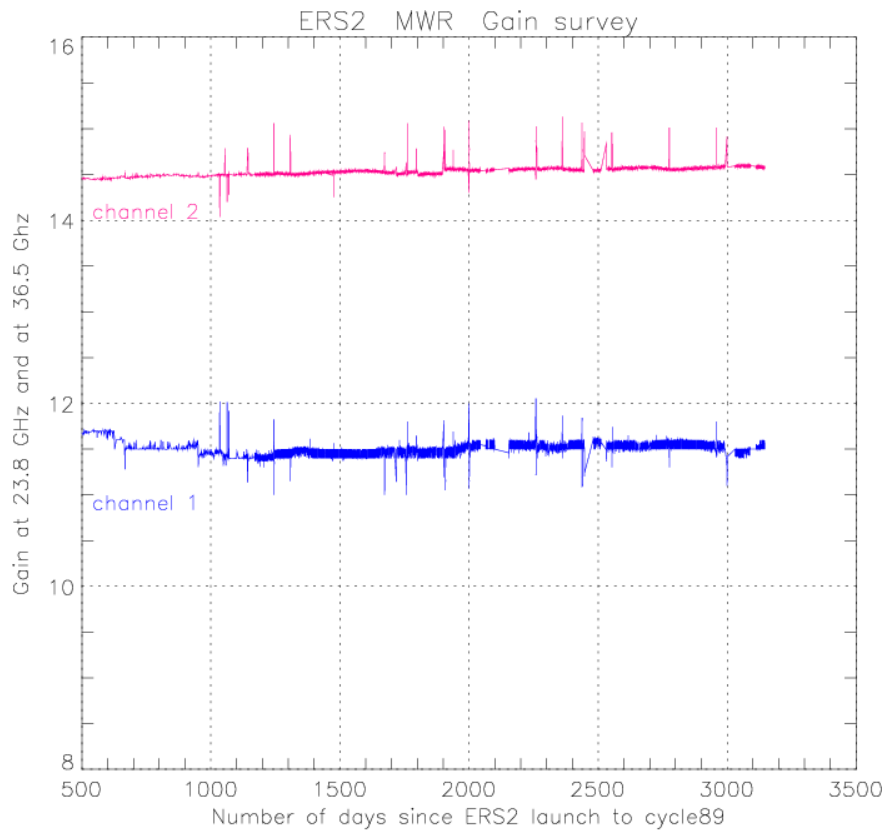


Figure 3: Time evolution of the gain since June, 1996.



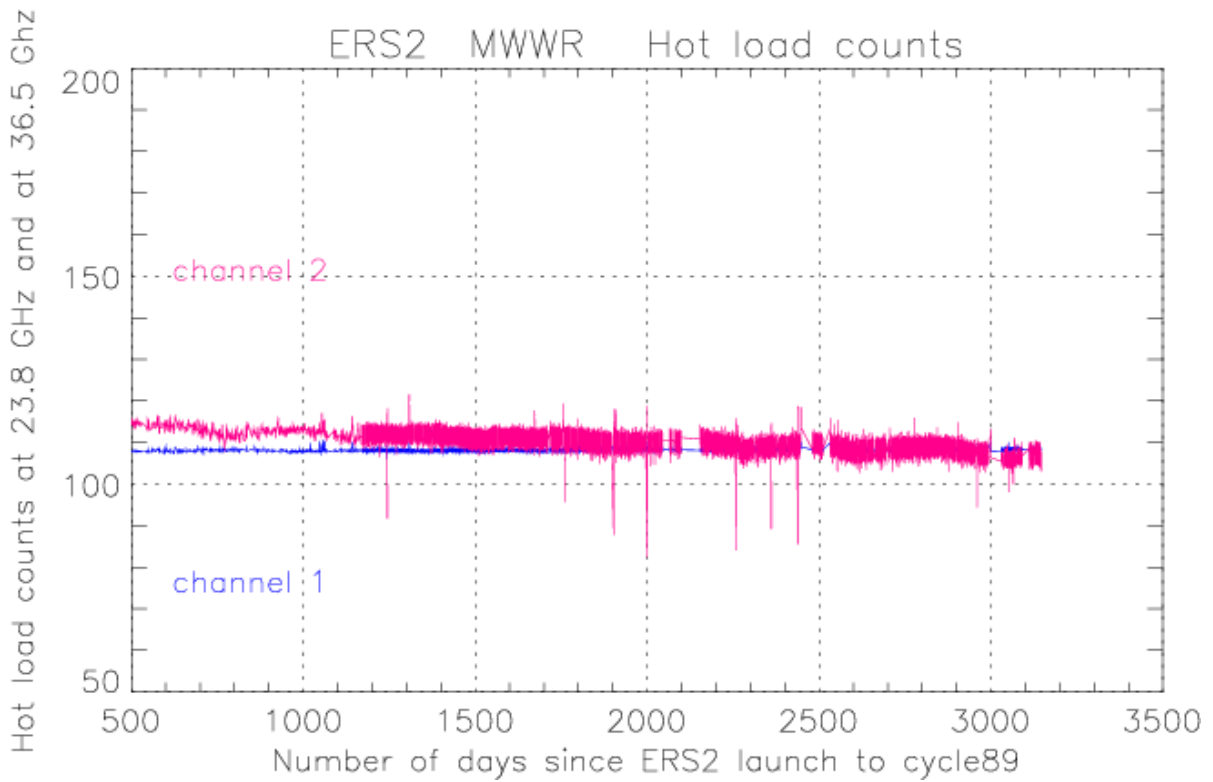
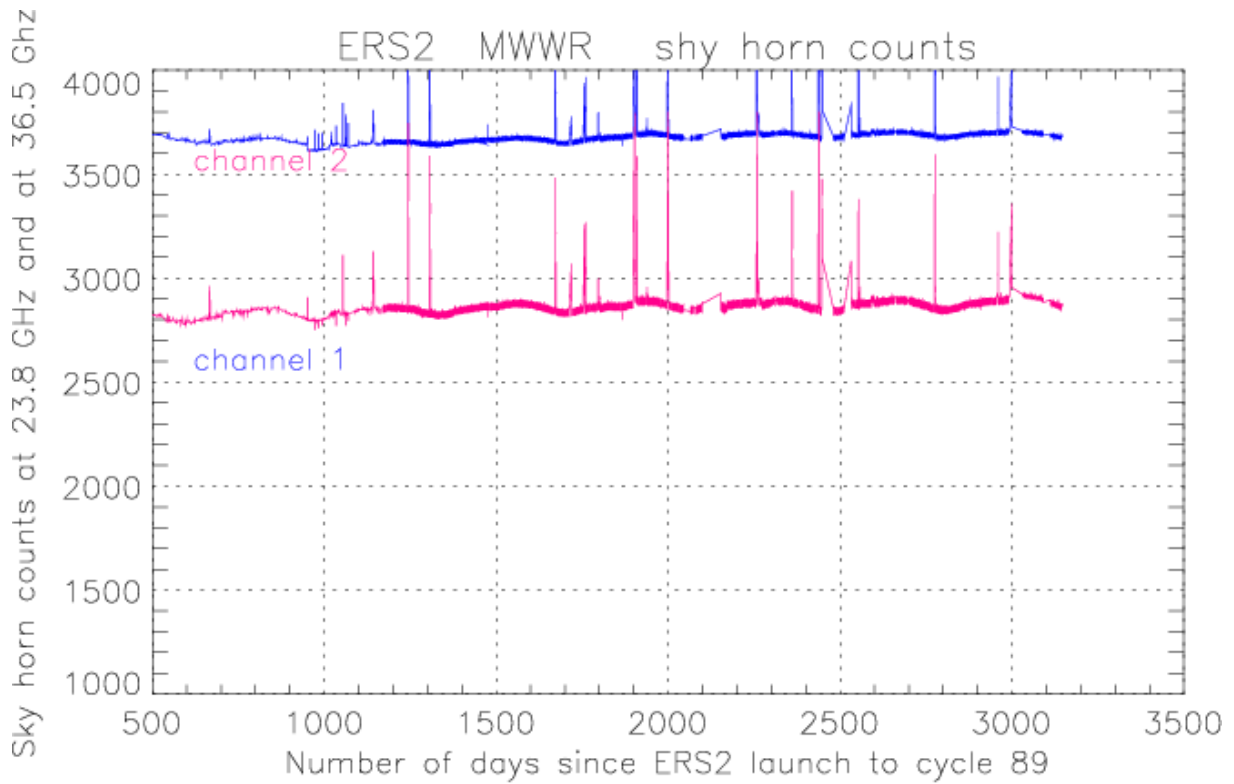


Figure 4: Time evolution of the sky horn count and the hot load count since June, 1996.

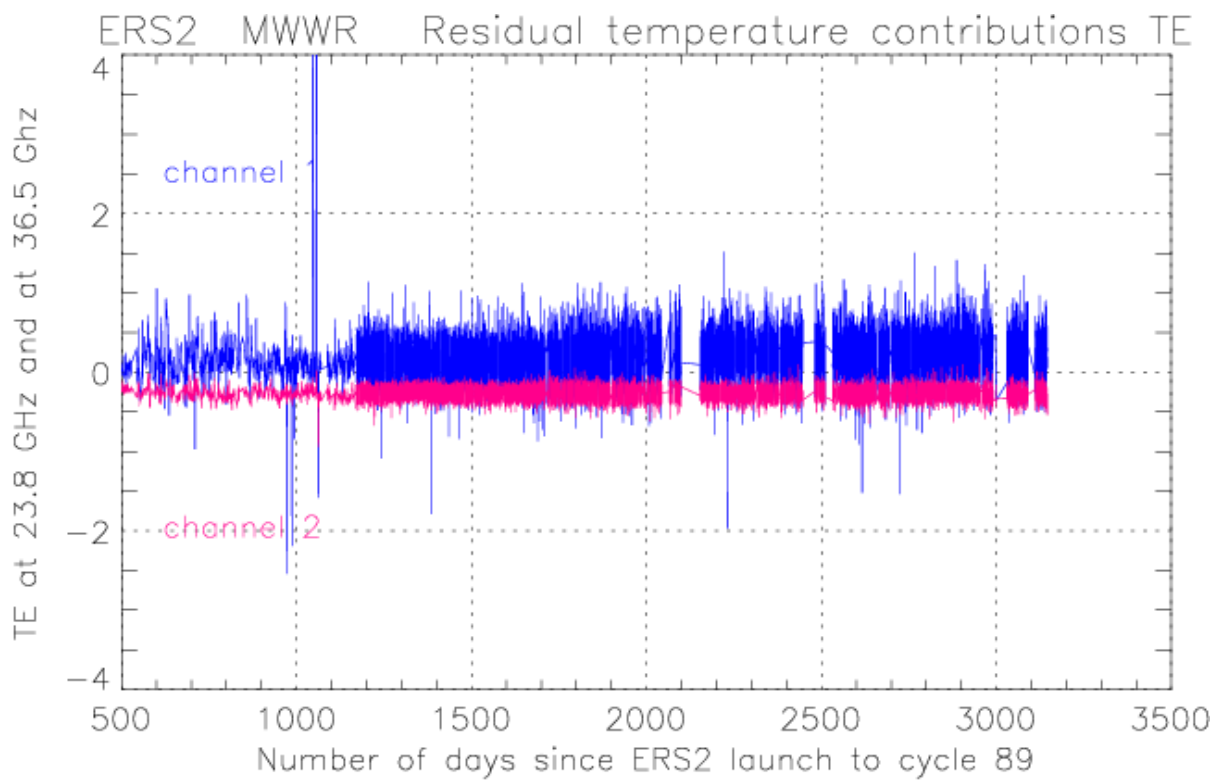


Figure 5: Time evolution of the residual temperature TE, since June, 1996.

## 4 Monitoring of cold ocean brightness temperatures

To assess the long term stability of the radiometer, monitoring of the two brightness temperatures was performed on several continental areas (Antarctic Plateau, South Greenland plateau, Amazon forest and Sahara desert) and by selecting the coldest measurements over ocean. The latter method, derived from Ruf's one for TMR (Ruf, 2000), was found to be the most efficient to point out the slight trend of channel A. the method consists of first filtering out data with value higher than a given threshold, then filtering out again the remaining data with values above the cycle average minus 1.5 times the standard deviation. The resulting time series is plotted in figure 6. Validation of the method was performed by checking its consistency on TMR data (in comparison with Ruf's results). The perfect stability of channel B is confirmed, and a trend is clearly depicted on channel A. The drift has been estimated to be -1.6 K between the gain drop in June 1996 and the end of September 2002 (date of the study performed by Eymard et al.) for low brightness temperatures (Obligis et al., 2003). For hot brightness temperatures, the long-term monitoring over hot continental areas (Amazon Forest and Sahara Desert) did not show any drift. This drift of channel A was also confirmed by comparing the MWR with TMR data at crossover points, and a linear correction is available (function both of time and brightness temperature, as it must vanish at the instrument physical temperature). This latter has been applied on the brightness temperatures corresponding to figure 6. Figure 7 shows the long-term monitoring of the 23.8 GHz brightness temperatures after applying the proposed correction.

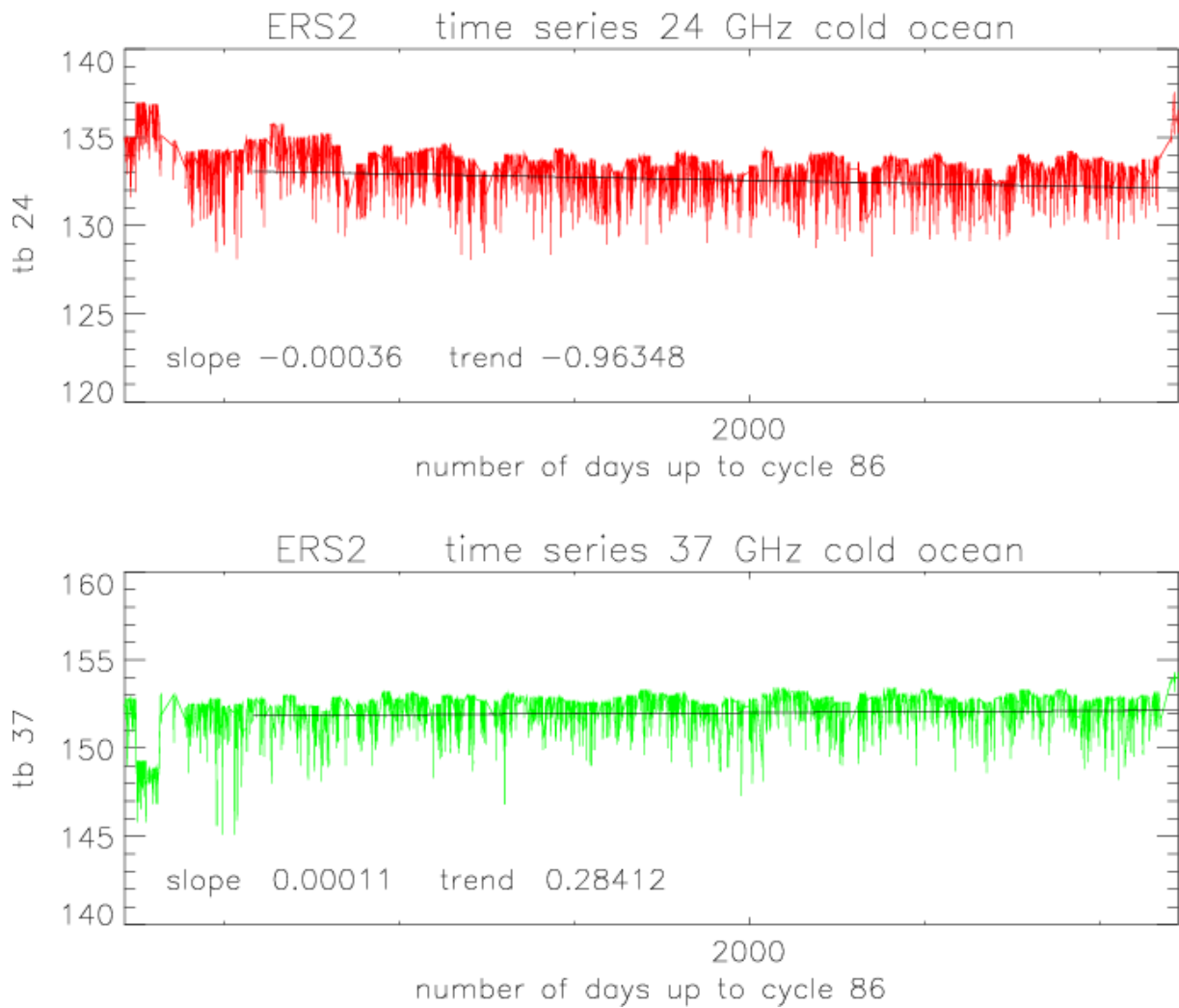


Figure 6: time series of the coldest brightness temperatures over ocean. Data are taken from launch to the cycle available at the time of the preparation of this report due to the use of the VLC tapes. Dates are referenced to January 1st, 1991.

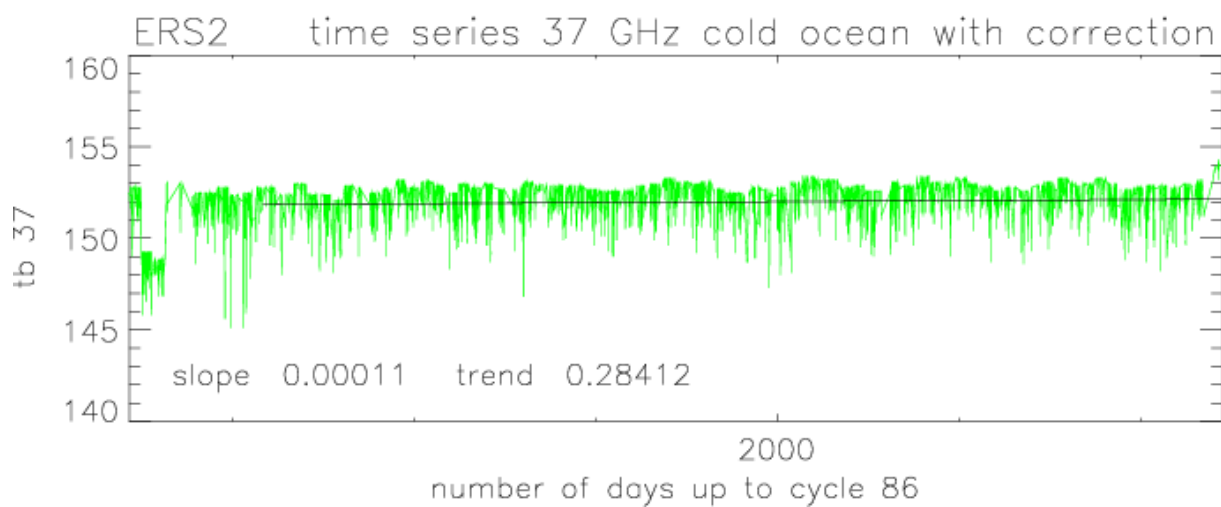
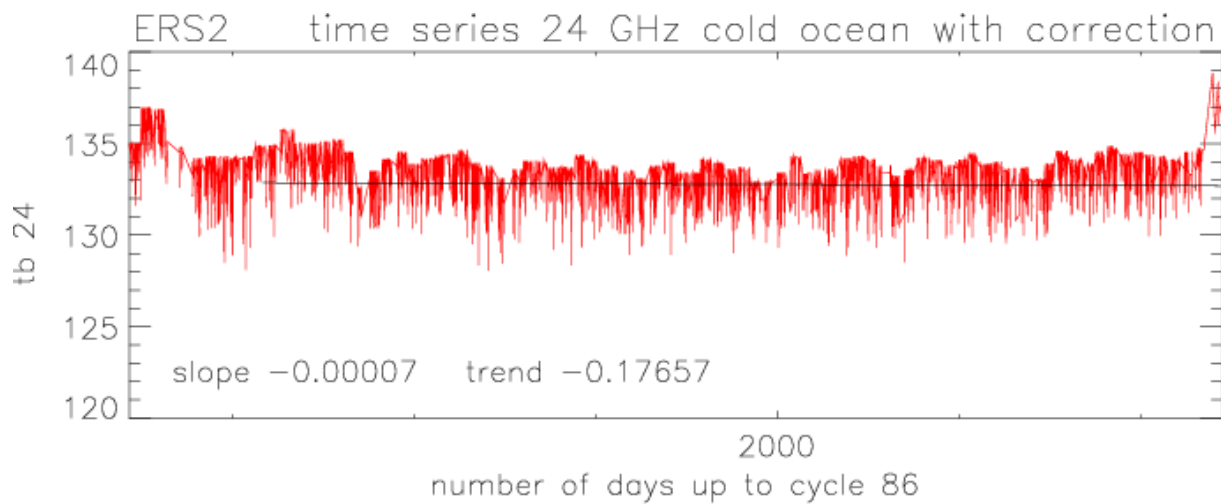


Figure 7: Same as figure 6 after correction of the 23.8 GHz TBs drift.

## 5 Conclusion on the cycle assessment and long term monitoring

The cycle 089 does not present any anomaly. Data gaps appear due to the recording problem. All internal parameters are nominal. The slight drift of channel A is constant and performances are still within the nominal limits. A linear correction is nevertheless available for the brightness temperature to allow the user to get a better stability of the tropospheric correction for the entire instrument lifetime. This latter seems to perform well. Note that in the cyclic reports up to cycle 088, there was a stretching of the time axis due to an anomaly in the routine used for the visualization of the monitoring of the coldest brightness temperature over ocean leading to the observation that the correction was a little bit too strong, it is now corrected and the proposed correction seems to perform well.

## 6 Reference documents

Bernard et al, The microwave radiometer aboard ERS-1: Part 1 - characteristics and performances, IEEE Trans. Geosci. Remote Sensing, 31(6), 1186-1198, 1993.

Eymard et al, Intercomparison of TMR and ERS/MWR calibrations and drifts, SWT TOPEX-JASON, New Orleans, Oct. 2002.

Eymard et al, Reports on activities performed in 2001 on the ERS2/MWR survey, May 2002.

Eymard et Obligis, Preliminary report on long-term stability of ERS2/MWR over continental areas, 1999.

Obligis et al, ERS2/MWR drift evaluation and correction, Feb. 2003.

Ruf, Detection of calibration drifts in spaceborne microwave radiometers using a vicarious cold reference, IEEE Trans. Geosci. Remote Sens., 38(1), 44-52, 2000.